

DIGITAL IMAGE CORRELATION ANALYSIS APPLIED TO MONITOR DAMAGE EVOLUTION OF COMPOSITE PLATES WITH STRESS CONCENTRATIONS AND BONDED PATCH REPAIRS

M.A. Caminero^{1*}, S. Pavlopoulou², M. López-Pedrosa², B.G. Nicolaisson³, C. Pinna²,
C. Soutis²

¹ Escuela Técnica Superior de Ingenieros Industriales, Universidad de Castilla-La Mancha, Campus Universitario s/n, 13071 Ciudad Real, Spain

²Department of Mechanical Engineering, The University of Sheffield, Sheffield, S1 3JD, UK

³Icelandair Technical Services, 235 Keflavik Airport, Iceland

* miguelangel.caminero@uclm.es

Keywords: Digital image correlation, Damage, Stress concentration, Bonded patch repair

Abstract

The use of composite materials in aircraft industry has risen significantly in recent years. During its service life, an aircraft is subjected to several structural and aerodynamic loads. These loads can cause damage or weakening of the structure that may affect its load carrying capabilities. The restoration of structural efficacy by repair or reinforcement of the damaged or weakened part to assure continued airworthiness of an aircraft has thus become an important issue in recent years. In this work, the behaviour of scarf-type bonded patches in laminate composites are monitored using full-field measurement methods based on Digital Image Correlation (DIC) techniques. Damage evolution of the repaired area under tensile loading was recorded from DIC and a Lamb wave based technique. These results were compared with X-radiographs and C-scan in order to identify damage after loading.

1 Introduction

The increasing use of high performance composite materials in the aerospace industry has risen significantly in recent years. For example, new age commercial aircrafts such as Boeing 787 and Airbus 350 are the first commercial aircraft to feature composites in fuselage primary structures [1]. Hence, there is an increasing need for repair technologies on primary structural components of the aircraft (such as the fuselage or the wings). Common damage on an aircraft can arise from accidental impact or from deterioration caused by the absorption of moisture or hydraulic fluid [2], [3]. Replacement of the damaged areas is not a preferable solution due to the high level of integration and the big size of the components. Therefore one of the common types of repair carried out with composite materials is adhesively bonded composite patch repairs [2]. The adhesive bonding of composite patches leads to cost effective and highly damage tolerant structural repairs in comparison with conventional mechanical fastened repair methods, usually riveting [3]. Most common types of repairs carried out with composites materials in aerospace industry are external patch repairs and scarf bonded repairs. These repair techniques differ from each other in terms of manufacturing and application. However, the performance and quality of a repaired structure using adhesive bonding depends not only in the bonding process, but also on the individual composite repair technician's experience

and skill. Hence, for such repairs to be certified by the Civil Aviation Authorities, on-line monitoring techniques are urgently needed.

Scarf repair technology provides certain advantages over the external patch technique. First of all it offers higher joint efficiency by matching ply to ply the original structure and by assuming uniform adhesive stresses along the scarf [2]. Moreover it provides a significant design advantage due to the fact that it does not change the aerodynamic properties of the structure and the disturbances are eliminated [4], [5]. However there are certain disadvantages that have to be considered before the implementation of a scarf repair such as the design procedure. First of all the manufacturing of a scarf repair requires a higher level of expertise than the external patch and it results to the removal of excessive amount of undamaged material for the achievement of a scarf angle that will ensure the stiffness and strength recovery [6]. Experimental studies show that adhesively bonded patch repairs can return the repaired surface to about 80% of the original undamaged laminate strength [7], [8], [9].

The mechanical behaviour of laminated composites is complex due to their specific features like heterogeneity and anisotropy. It is therefore more desirable when doing experimental investigation on laminated composites to obtain extensive full-field experimental data, rather than limited strain or displacement measurements from strain gauges or extensometers [10], [11], [12]. This is especially relevant when experimentally evaluating composite repairs, since it is important to monitor the whole repaired area in order to conclude on the repair mechanical behaviour under loading conditions. From the literature review, it seems that rather limited use of full-field data to assess the performance of composite repairs under loading has been applied in the past. However, infrared thermography (IRT) has been used for structural reliability inspection of composites patches [13], and for detecting damage initiation and progression in repaired specimens under tensile fatigue loading in order to assess the damage initiation of the repairs [3]. In order to monitor the damage process of composite laminates specimens, digital image correlation (DIC) technique has been applied, which is convenient for full-field strain measurements, in previous studies [10], [11], [12], [14], but only a limited number of studies focused on the performance of patch repaired composite structures has been applied before, see for example reference [9], [15], [16]. Furthermore, a non-destructive testing method based on Lamb waves for damage detection in the composite specimen has been successfully used in the past for fault and damage detection in repaired laminated composite structures [17], [18], [19], [20], [21].

In this work the assessment of the damage taking place under uniaxial tension in open-hole specimens and adhesively bonded patch repairs in composite structures is examined. Understanding of notched specimen behaviour is necessary for the design of complex structures where different parts are mostly connected with bolts and rivets. A scarf patch repaired was performed on an impact damaged woven carbon-fibre epoxy M21/HTA panel. Tensile tests are carried out in order to study damage evolution and performance of the bonded patch repair. In order to monitor the failure process of the repaired area during loading, 2-D and 3-Dimensional Digital Image Correlation (DIC) techniques are applied along with guided Lamb waves analysis (on-line techniques). Damage evolution of the repaired area under tensile loading is recorded from DIC and the Lamb waves based technique. The correlation of the extracted features using both on-line techniques and the stage damage is also discussed. Finally the study compares results from the on-line analysis and from off-line techniques such as ultrasonic C-scanning and X-ray radiography in order to identify damage after loading.

2 Experimental and Materials

2.1 Material and specimen preparation

A scarf patch repair was performed on an impact damaged carbon-fibre reinforced plastic (CFRP) panel, see Figure 1. At the front face, a hole of approximately 13 mm in diameter appeared whereas the total damaged area on the back face was close to 25 mm long \times 25 mm wide.

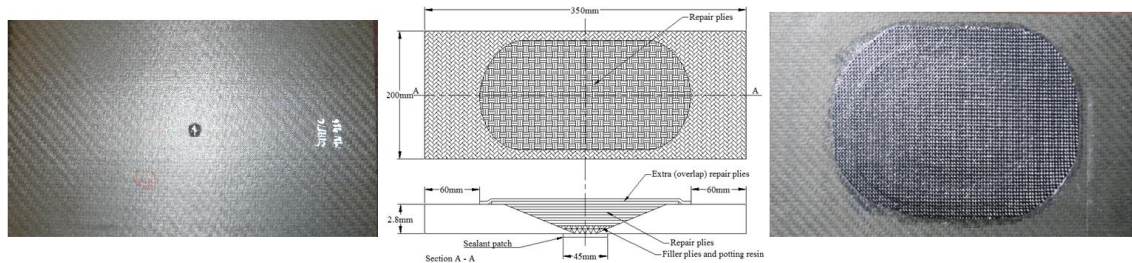


Figure 1. Left: CFRP panel after impact. Center: Scarf repair geometry details. Right: Cured scarf repair specimen

The panel was made out of woven (2/2 twill) carbon fibre (HTA) with toughened epoxy resin system (M21) supplied by Hexcel Composites and moulded by Hurel-Hispano UK at a nominal 58% fibre volume fraction. The panel's lay-up sequence was $[0/90/\pm 45/0/90]_3T$ and its total thickness was 2.8 mm. After the impact testing, the panel was prepared by drilling a circular hole at the centre of the specimen in order to simulate the result of clearance of damaged region. The scarf repair was made out of an aerospace qualified composite material and the manufacturing procedure followed the Boeing 767 Structural Repair Manual [22]. Several specimens were cut from the panel in order to obtain the material unnotched and notched tensile strength and the elastic material properties. The averaged experimental results (using three unnotched and notched tensile specimens) for the composite system HTA/M21 in terms of ultimate tensile strength are shown in Table 1. We consider quasi-isotropic behaviour in the x-y laminate plane.

| HTA/M21 (0/90/ \pm 45/0/90) _{3T} | Measurements |
|--|--------------|
| Unnotched tensile strength (σ_{un}) | 585 MPa |
| Notched tensile strength (σ_n) | 379 MPa |
| Elastic Modulus (E_x) | 49.4 GPa |
| Poisson's Ratio (ν_{xy}) | 0.26 |
| Shear Modulus (G_{xy}) | 19.6 GPa |

Table 1. Tensile strength of unnotched and notched specimens and elastic properties of HTA/M21

2.2 On-line damage monitoring using Digital Image Correlation (DIC)

One of the major limitations that apply to the use of repair patches in aerospace industry is the risk of debonding of the patch under loading in critical stages of the structure's life. This can occur if the ultimate shear strain of the adhesive is exceeded under loading. In the current study, two non-destructive testing (NDT) methods have been used for the on-line damage monitoring of the patch repaired composites: Digital image correlation (DIC) technique, which is convenient for full-field strain measurement and Guided ultrasonic waves (Lamb waves), that belongs to the Structural Health Monitoring (SHM) category.

Digital Image Correlation (DIC) is a non destructive optical method, which estimates the 2-dimensional (2D) or 3-dimensional (3-D) displacements and strain fields of an object. The main principle of this method is to match the speckle pattern that covers the surface of the tested specimens before and after the loading. This leads to a random structured aspect, which

can be observed with a digital camera. In comparison with other experimental techniques such as Moiré interferometry and electric speckle interferometry, DIC is simple and robust because complicated surface treatment is not needed and its requirement for testing environment is low [4], [23]. The 3D system is more sufficient since it allows the measurement of the three dimensional displacement fields simultaneously. Furthermore, it works on non-flat surfaces and is not affected by large rigid body movements.

The images used in the experiments were obtained by two digital cameras with a CCD matrix of more than five million pixels; model DCP 5.0 LIMESS Messtechnik & Software GmbH. The typical error of displacement measurement is less than 0.05 pixels, and that of strain measurement is less than 500 μm . The experimental data obtained in this study were processed with Vic-2D and -3D software from Correlated Solutions, Inc. The specimens were prepared with white painting and sprayed with a black aerosol to create a random speckle pattern. The specimen was illuminated by ordinary white light in the experiment.

3 Results and Discussion

3.1 Open-hole tensile specimen

DIC technique was used to provide full-field strain measurements of the surface of a notched (open hole) woven HTA/M21 carbon fibre specimen (175 mm long \times 50 mm wide with a hole diameter of 5 mm) loaded in tension. Prior to the DIC experiment, the specimen was loaded at 80% (42.4 kN) and 90% (47.7 kN) of its ultimate tensile strength (\approx 53 kN) and then X-ray radiography was used as an inspection method in order to compare the results obtained from the DIC strain measurements.

Figure 2 (Left) depicts X-ray radiographs at different loading stages of the notched specimen. The results show different types of damage near the hole, as 45° and 90° off-axis matrix cracks (matrix cracking) and 0° splits (splitting). The results also show a non-symmetric damage development around the hole: the left side the hole presents higher failure than the right side. This effect may be partly based on different factors as, for example, a misalignment of the specimen during the loading process, thickness variation of the specimen or a non-uniform loading of the specimen.

In order to prepare the test specimen for the DIC experiment, a speckle pattern was prepared on the specimen surface using airbrush and white paint. The quality of the speckle pattern (random size and distribution) was analyzed. The specimen was tested in tension. The images were recorded using Vic-Snap software from Correlated Solutions, Inc with a rate of 1 image per second and a spatial resolution of 0.016 mm/pixel. The experimental data obtained in this test were processed with Vic-2D software from Correlated Solutions, Inc. Correlation subsets of 32 pixels with a step size of 5 pixels were selected to perform DIC calculation. This subset size was large enough to ensure that there is a sufficiently distinctive pattern contained in the area used for correlation. Figure 2 (Right) shows DIC results in terms of Hencky strain plots at the same loading stages than the previous analysis. The results show high strain concentrations ($\epsilon_{\text{max}} = 0.0349$ for 80% of the UTS and $\epsilon_{\text{max}} = 0.0551$ for 90% of the UTS) taking place at the hole boundaries, especially at the left hand side where 0° splits and 90° off-axis matrix cracks have initiated, as observed on the X-ray radiographs in Figure 2. The comparison of measured strain fields with observed damage using X-ray radiographs has demonstrated that the shift in the strain distributions and high strain regions ($\sigma_{\text{max}} \gg \sigma_{\text{unnotched}}$) are directly linked to the different types of damage (splitting, matrix cracking) occurring around the hole and therefore predict where crack growth is taking place.

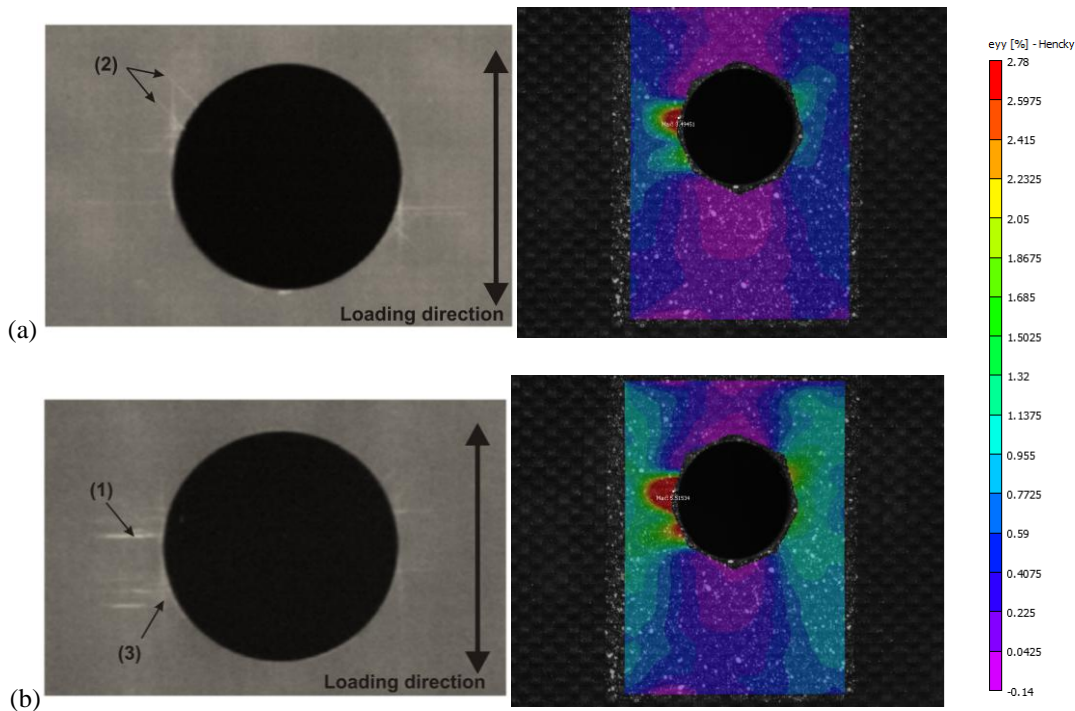


Figure 2: (Left) X-ray radiographs showing different stages of notched HTA/M21 specimen loaded in tension. (a): 80% (42.4 kN) of UTS (≈ 53 kN) and (b) 90% (47.7 kN) of the UTS. (1) and (2) indicate 90° and 45° off axis matrix cracks and (3) 0° splits. (Right) DIC Hencky strain results at the same loading stages. (a) 80% of the UTS ($\epsilon_{\max} = 0.0349$) and (b) 90% of the UTS ($\epsilon_{\max} = 0.0551$)

3.2 Scarf repaired specimen

The scarf repaired panel was sprayed with a random speckle pattern to enable the image recording with the DIC technique. The specimen was illuminated by ordinary white light. Also eight piezoelectric transducers (PZT) were surface mounted on the panel operating in pitch catch mode, forming 16 propagation paths and hence covering all critical areas, see Figure 3.

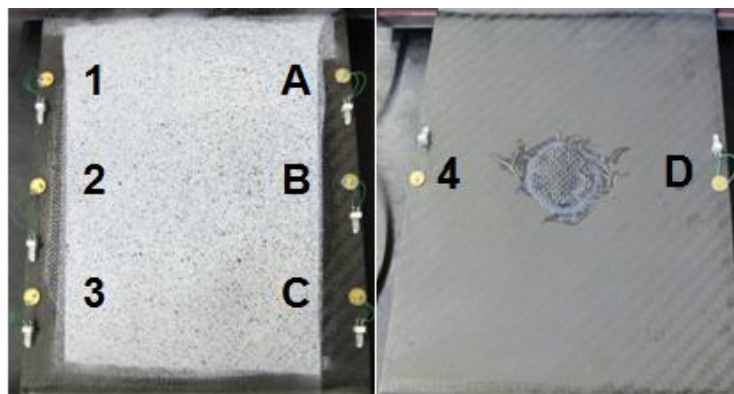


Figure 3: Scarf repaired with speckle pattern and PZT transducers. Propagation paths: Actuators: 1,2,3,4 and Receivers: A,B,C,D

As a first step, readings from the healthy condition were recorded before any loading was applied. These were considered to be the "baseline reference". In addition, the camera system was calibrated using a uniformly spaced dot pattern with 15 mm spacing. The specimen was loaded in quasi-static tension and Lamb wave signals and DIC images were recorded at 10-20 kN up to 170 kN. At this load, the panel failed prematurely due to cracks that initiated around

the holes that were drilled for gripping the specimen. Nevertheless, for the characterisation of the panel with the two investigated methods the amount of data that was collected was sufficient for reaching some useful conclusions in relation to damage monitoring. The images obtained in this test were processed with Vic-3D software from Correlated Solutions, Inc. The subset size was selected large enough to ensure that there is a sufficiently distinctive pattern contained in the area used for correlation. The 3D DIC analysis provided full-field strain maps of the repaired area for all the considered loading cases. The interesting strains were the ones obtained in the loading direction (ϵ_{yy}). The results of the most representative load levels are illustrated in Figure 4.

The tensile strength of the scarf repair is expected to be between the tensile strength of the unnotched and the notched sample. However for precision purposes, it is well accepted that the optimum patch configuration can recover 70-80% of the laminate's undamaged strength. Therefore the maximum tensile strength of the scarf repair can be estimated to be approximately between 409-468 MPa. In addition there are several factors that can lead to lower strength such as the discontinuities introduced during the manufacturing process. According to the estimation of the maximum stress that developed at 170 kN locally around the hole, the stress was 415 MPa which is close to the failure stress of the repaired panel. This value was measured through the strain analysis of the DIC figures at an applied load of 170 kN. The current analysis concludes that it is quite possible that even though the load did not reach the ultimate strength of the scarf repair due to the premature grip failure, local internal damage is expected to develop. This assumption is well supported both from the DIC figures and the Lamb wave's analysis.

Lamb waves were recorded for all load levels until the panel failed. The position of the transducers was decided to be outside the repair area since debonding of the upper ply of the patch was expected and hence there was a possibility of the transducer losing contact with the tested surface. The peak to peak amplitude is defined as a simple damage index for assessing the structural integrity of the scarf repair and for taking into consideration the multiple propagation paths. In Figure 5 the damage index is illustrated for the different levels of loading.

For the purposes of the current work the damage index was analyzed and its sensitivity was correlated with the recorded DIC images and with the interaction of each path with the geometrical features. First of all, the damage index drops after 120 kN for specific propagation paths and after 140 kN almost for all propagations paths. This phenomenon is in good agreement with the fact that after 120 kN and more precisely after 140 kN, DIC images captured deformations that occurred mostly around the hole of the substrate but also in several places on the patch plies (capturing discontinuities and possible failure modes in the form of resin cracking). Furthermore paths 3A and 3C show a relatively higher change in terms of the damage index than the rest of the analyzed paths especially after 140 kN. The respective DIC figure for this load level has captured high strains at the end of the patch under the hole and close to the grips. Therefore the developed changes in the damage index can be justified. Path 2D directly propagated through the resin filled hole where high level of deformation and initiation of internal cracks were more likely to happen. The behaviour of the damage index for this path is relatively steady up to 120 kN and then it considerably drops which again can be justified by the developed strain field around the hole. Paths 2C and 4C show very similar behaviour as it was expected since they propagate through the same direction only on different sides of the panel. Finally the damage index sensitivity of the path 1A can be explained if it is taken into consideration that the panel failed in the grips of the upper part, so that path was probably affected by the high stress distributions at that area.

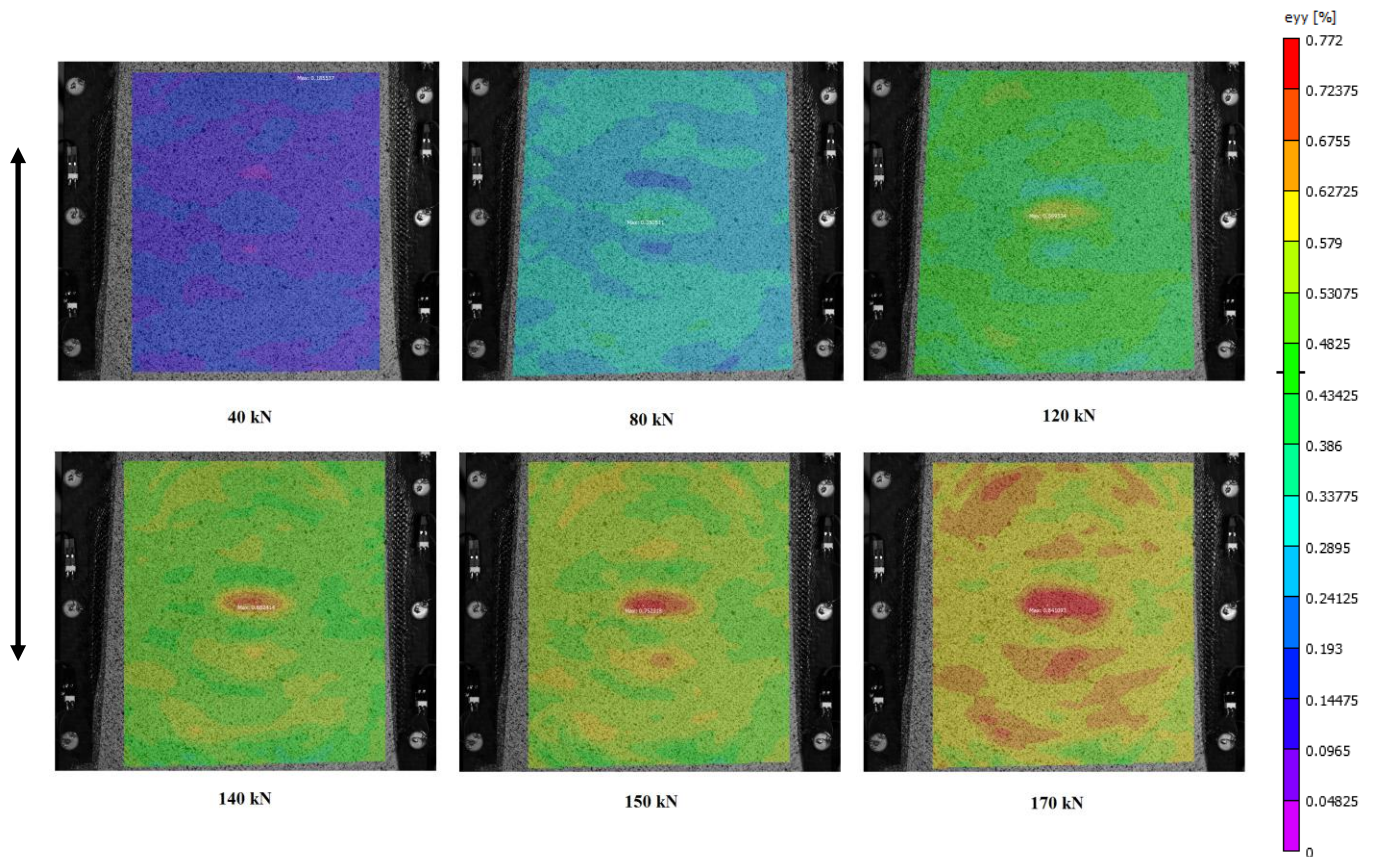


Figure 4: Full-field DIC results: Strain distribution at the surface of the repaired area in the loading direction (ϵ_{yy}) at different loading stages: 40, 80, 120, 140, 150 and 170 (failure) kN

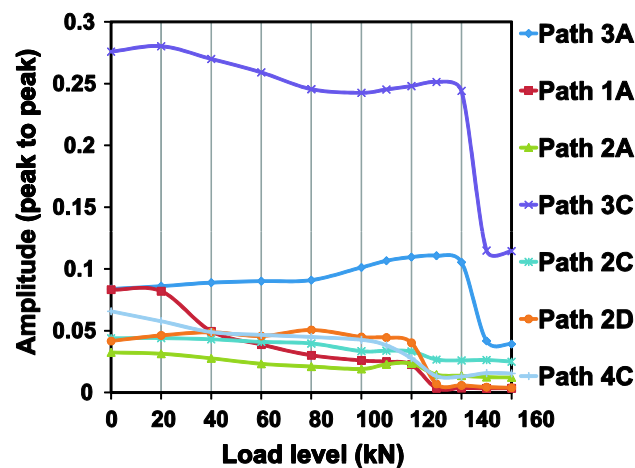


Figure 5: Damage index (peak to peak) with respect to the load level

Within the purposes of the current work, different methods were compared for the identification of their damage sensitivity in early damage stages. As a result ultrasonic C-scan and X-ray radiographs tests were performed for the characterization of the panel after its failure but no evidence of permanent damage was shown. However it is common in composite structures, that early stage damage, like internal delaminations and intralaminar resin cracks that have not reached critical lengths yet, can close after unloading. This observation highlights the advantage of in-situ monitoring (DIC and Lamb Waves) for capturing internal damage in early stages which could be catastrophic especially for composite structures and

which might not be captured by the traditional off-line testing techniques such as C-scanning and X-ray radiographs.

4 Conclusions

The aim of this study was to assess the use of DIC techniques for damage detection on bonded composite repairs. DIC technique was successfully used to detect damage process in composite systems. First, 2D-DIC technique was used to obtain full-field strain measurements in open-hole tensile CFRP specimens and X-ray radiographs were performed to identify the damage localized around the hole. It has been shown that cracks were easily picked up by the DIC technique and a comparison of measured strain fields with observed damage using X-rays has demonstrated that the shift in the strain distributions and high strain concentrations are directly linked to different type of damage (splitting, matrix cracking) around the hole. On the other hand, a scarf repair was tested under tensile loading and its damage assessment was performed with 3D-DIC and Lamb waves. The comparison between both techniques showed a great accordance.

Results have shown the potential of the investigated methods for the on-line monitoring (DIC and Lamb waves) of scarf repairs in aerospace applications. The DIC technique is revealed to be an efficient and simple methodology to study damage on bonded composite repairs. Lamb waves as a structural health monitoring technique provides certain advantages over DIC method since it could be potentially implemented as a built-in sensing technique during the manufacturing of the panel. Moreover the current work highlights the inefficiency of off-line monitoring techniques (C-scanning and X-rays) for early damage cases in materials where the propagation of damage could be catastrophic especially for composite structures.

References

- [1] Gardiner G., Primary structure repair: The quest of quality. *High Performance Composites*, (2011).
- [2] Hu F.Z., Soutis C., Strength prediction of patch-repaired CFRP laminates loaded in compression. *Composites Science and Technology*, **60**, pp. 1103-1114 (2000).
- [3] Cheng P., Gong X.J., Hearn D., Aivazzadeh S., Tensile behaviour of patch-repaired CFRP laminates. *Composite Structures*, **93**, pp. 582-589 (2011).
- [4] Hart-Smith L.J., Adhesively-bonded scarf and stepped-lap joints, *NASA Technical Report CR 112237*, (1973).
- [5] Oplinger D.W., *Mechanical fastening and adhesive bonding*, in "Handbook of Composites", edited by S.T. Peters, Chapman & Hall, London, pp. 610-666.(1998)
- [6] Whittingham B., Baker A.A., Harman A., Bitton D., Micrographic studies on adhesively bonded scarf repairs to thick composite aircraft structure, *Composites Part – A*, **40**, pp. 1419–1432, (2009).
- [7] Soutis C., Hu F.Z., *Design and performance of bonded patch repairs of composite structures*, in *Proceedings of the Institution of Mechanical Engineers, Part G: Journal of Aerospace Engineering*, **211**, pp. 263-271 (1997).
- [8] Breitzman T.D., Iarve E.V., Cook B.M., Optimization of a composite scarf repaired patch under tensile loading, *Composites: Part A*, **40**, pp. 1921-1930, (2009).
- [9] Holzhüter D., Sinapius M., Infusion Technology for Bonded CFRP Repairs for Aircraft Primary Structures, *German Aerospace centre (DLR)*, Braunschweig (Germany), (2011).
- [10] Grediac M., The use of full-field measurement methods in composite material characterization: interest and limitations, *Composites: Part A*, **25**, pp. 751-761. (2004).
- [11] Pierron F., Green B., Wisnom M.R., Hallet S.R., Full-field assessment of the damage process of laminated composite open-hole tensile specimens. Part I: Methodology, *Composites: Part A*, **38**, pp. 2307-2320, (2007).

- [12]Lagattu F., Lafarie-Frenot M.C., Lam T.Q., Brillaud J., Experimental characterization of overstress accomodation in notched CFRP composite laminates, *Composite Structures*, **67**, pp. 347-357, (2005).
- [13]Avdelidis N.P., Moropoulou A., Marioli-Riga Z.P., The technology of composite patches and their structural reliability inspection using infrared imaging, *Progress in Aerospace Sciences*, **39**, pp. 317-328, (2003).
- [14]Pierron F., Green B., Wisnom M.R., Hallet S.R., Full-field assessment of the damage process of laminated composite open-hole tensile specimens. Part II: Experimental results, *Composites Part A*, **38**, pp. 2312-2332, (2007).
- [15]Sutter D.A., Three-dimensional analysis of a composite repair and the effect of overply shape variation on structural efficiency, *Msc Thesis, Department of the air force, Air Force Institute of Technology USA*, (2007).
- [16]Nicolaïsson B.G., Analysis of adhesively bonded repairs in composite structures, *Msc Thesis, Department of Mechanical Engineering, The University of Sheffield UK*, (2011)
- [17]Diamanti K., Soutis C., Hodgkinson J.M., Non-destructive inspection of sandwich and repaired composite laminated structures, *Composite Science and Technology*, **65**, pp. 2059-2067, (2005).
- [18]Soutis C., Ihn J-B., *Design, analysis and structural health monitoring of bonded composite repair and substrate*, in “Encyclopaedia of Structural Health Monitoring”, edited by C. Boller, F.K. Chang, Y. Fujino, John Wiley and Sons Ltd, (2009).
- [19]Diamanti K., Soutis C., Structural health monitoring techniques for aircraft composites structures, *Progress in Aerospace Sciences*, **46**, pp. 342-352, (2010).
- [20]Pavlopoulou S., Soutis C., Manson G., Non-destructive inspection of adhesively bonded patch repairs using Lamb waves, *Plastics, Rubber and Composites*, **41**, pp. 61-68, (2012).
- [21]Pavlopoulou S., Soutis C., Staszewski W.J., *Structural health monitoring of composite scarf repairs with guided waves* in “Proceeding of the 2nd International Workshop on Smart Diagnostics of Structures”, Krakow, Poland, (2011).
- [22]Boeing, *767-300 Structural Repair manual SRM*, Boeing, Seattle, USA (2011)
- [23]Wang Z.Y., Li H.Q., Tong J.W., Sheng M., Aymerich F., Priolo P., Dual magnification digital image correlation based strain measurement in CFRP laminates with open hole, *Composite Science and Technology*, **68**, pp. 1975-1980, (2008).